

Phenoxazinone synthase activity of a mononuclear cobalt(III) complex

Merry Mitra & Rajarshi Ghosh*

Department of Chemistry, The University of Burdwan,
Burdwan 713 104, India

Email: rghosh@chem.buruniv.ac.in

Received 19 October 2015; revised and accepted 17 May 2016

The trivalent cobalt complex, $[\text{Co}(\text{HL})_2](\text{OAc})\cdot\text{H}_2\text{O}$ (**1**) [$\text{H}_2\text{L} = N$ -(2-hydroxyethyl)-3-methoxysalicylaldimine], behaves as an effective catalyst towards oxidative dehydrogenation of *o*-aminophenol to 2-aminophenoxazine-3-one in aerial oxygen. The reaction follows Michaelis-Menten enzymatic reaction kinetics in methanol with turnover number ($K_{\text{cat}} = 2.83 \times 10^3 \text{ h}^{-1}$).

Keywords: Coordination chemistry, Metalloenzymes, Dehydrogenation, Oxidative dehydrogenation, Phenoxazinone synthase activity, Cobalt, Michaelis-Menten kinetics

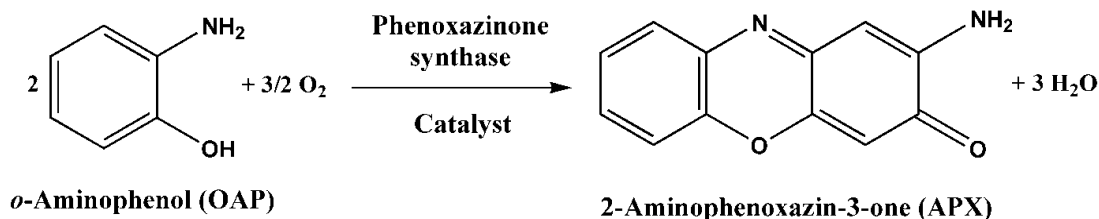
Metalloenzymes that activate molecular oxygen possess great potential as catalyst for specific oxidation reactions and as guides for the development of efficient small molecule catalysts¹⁻⁶. These low-molecular metal complexes serves as functional model and catalyze the same (or a closely related) reaction as does the metalloenzyme to be mimicked. In combination with the structural models which mimic various structural features, functional models constitute the basis for the modelling approach in the study of metalloenzymes, which regards metalloenzyme active sites as metal complexes embedded in a protein matrix. The study of biomimetic reactions catalyzed by functional metalloenzyme models helps to understand the mechanisms of metalloenzyme action and assists the design of metal complex catalysts for specific purposes (bioinspired catalysis)⁷.

The enzyme, phenoxazinone synthase, a type 2 copper-containing oxidase (subunit molecular mass 88,000, 3.7 Cu per subunit)⁸ is naturally found in the bacterium *Streptomyces antibioticus* and has been cloned and over expressed in *S. Lividians*⁹. This enzyme catalyzes the six electron oxidative coupling of two molecules of a substituted 2-aminophenol to the phenoxazinone chromophore (Scheme 1) in the final step in the biosynthesis of actinomycin D, namely, the oxidative condensation of two molecules of 3-hydroxy-4-methylanthranilic acid pentapeptide lactone to form actinocin (Scheme 2)¹⁰. Actinomycin D is clinically used to treat Wilm's tumor, gestational choriocarcinoma, and other tumors¹¹⁻¹³.

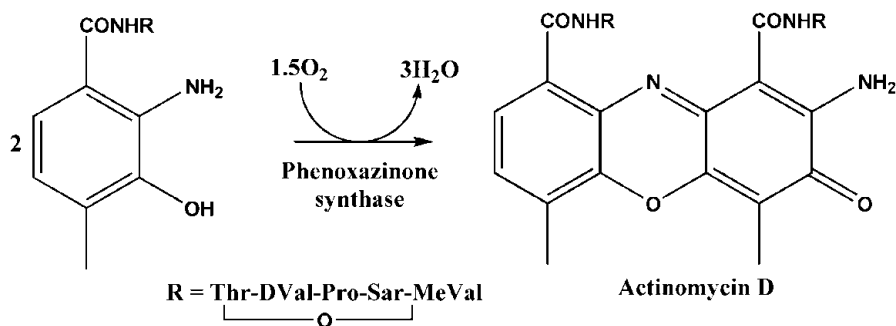
The synthesis and reactivity studies of transition metal complexes, as model compounds for metalloenzymes with oxidase (oxygenase) activity, are of particular interest for the development of bioinspired catalysts for oxidation reactions. Several copper(II)¹⁴, cobalt(II/III)¹⁵, manganese(II/IV)¹⁶, iron(III)¹⁷ complexes as functional models of phenoxazinone synthase have been reported. Herein, we report the phenoxazinone synthase activity of a trivalent cobalt(III) complex, $[\text{Co}(\text{HL})_2](\text{OAc})\cdot\text{H}_2\text{O}$ (**1**) [$\text{H}_2\text{L} = N$ -(2-hydroxyethyl)-3-methoxysalicylaldimine], which has been structurally characterized by X-ray data earlier (Fig. 1)¹⁸. (**1**) behaves as an effective catalyst towards oxidative dehydrogenation of *o*-aminophenol (OAPH) to 2-aminophenoxazine-3-one (APX) in aerial oxygen.

Experimental

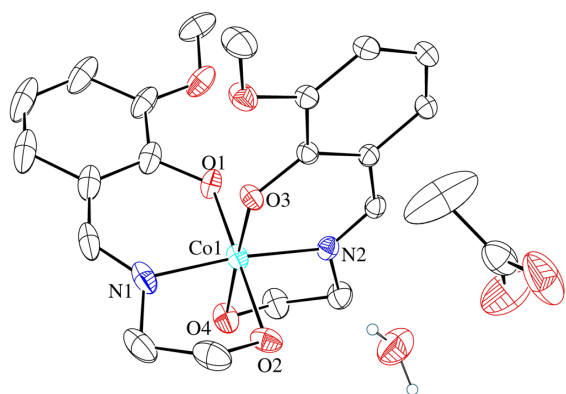
High purity *o*-vanillin (Aldrich, UK), 2-aminoethanol (Aldrich, UK), cobalt(II) acetate tetrahydrate (Aldrich, UK), *o*-aminophenol (Aldrich, UK) and all other solvents were purchased from the respective concerns and used as received. Solvents were dried according to standard procedure and distilled prior to use.



Scheme 1



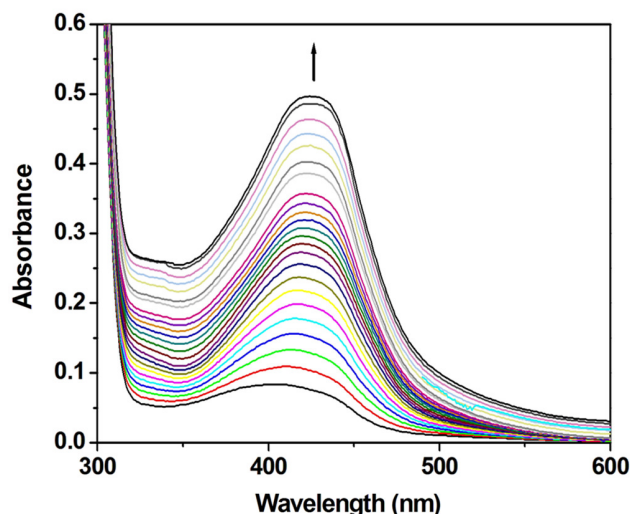
Scheme 2

Fig. 1—ORTEP of $[\text{Co}(\text{HL})_2](\text{OAc})\cdot\text{H}_2\text{O}$ (**1**).¹⁸

UV-vis was recorded using a Shimadzu UV-vis 2450 spectrophotometer. Mass spectrometric data were collected on Xevo G2 Q TOF mass spectrometer using electron spray ionisation (ESI) techniques.

Results and discussion

Solution of (**1**) was treated with 100 equivalents of OAPH under aerobic conditions. The repetitive UV-Vis spectral scan was recorded in pure MeOH (Fig. 2). The time dependent spectral scan shows very smooth growing of APX band at 427 nm. APX was identified by HRMS with $m/z = 212.0585$ (Fig. 3). In order to find out the comparative reaction rate between OAPH and (**1**), the reaction kinetics between (**1**) and OAPH were studied by observing the time dependent change in absorbance at a wavelength of 427 nm. The colour of the solution gradually turned deep brown, indicative of gradual conversion of OAPH to APX. The difference in absorbance (ΔA) at 427 nm was plotted against time to obtain the initial rate for that particular catalyst to substrate concentration ratio (Fig. 4). A first-order catalytic reaction was observed, with initial rate = 0.03787 min^{-1} . The average rate of the reactions shows that the rate is first order at the region of low concentrations of the substrate, OAPH,

Fig. 2—Changes in spectral pattern of complex (**1**) in MeOH after reaction with OAPH. [Reaction time: 6 h].

and zero order at its higher concentrations (Supplementary data, Fig. S1). This observation indicates that the oxidation of OAPH proceeds through the formation of a relatively stable intermediate, which is a complex-substrate adduct, $[\text{Co}(\text{HL})_2]\text{-OAP}\cdot\text{H}_2\text{O}(\text{Na}^+)$, with $m/z = 597$ (Supplementary data, Fig. S2), presumably formed by expanding the coordination number of the cobalt(III) in (**1**).

A probable reaction mechanism as well as catalytic cycle for the formation of phenoxazinone chromophore is given in Scheme 3. In the first step, OAPH forms an adduct with the Co(III) complex (**1**), (**1a**· $\text{H}_2\text{O}\text{-Na}^+$), having $m/z = 597$, as shown by mass spectrometry (Supplementary data, Fig. S2). This adduct generates the OAP radical by reacting with molecular oxygen¹⁹. The liberated H_2O_2 in this step was estimated spectrophotometrically (See Supplementary data). The OAP radical forms *o*-benzoquinone monoamine, which on oxidative dehydrogenation reaction involving OAPH and molecular oxygen, produces 2-amino-phenoxazine-3-one (Scheme 3).

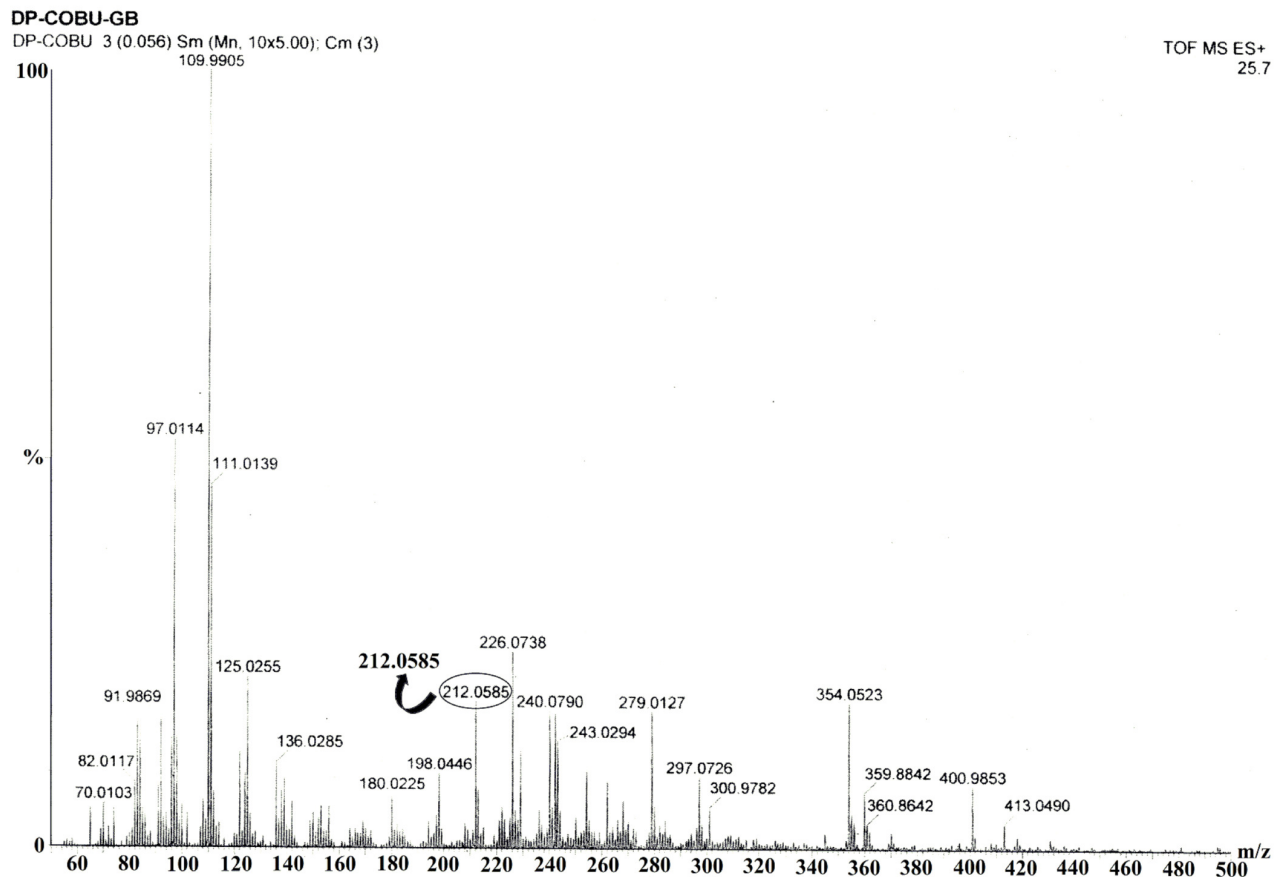


Fig. 3—ESI-MS spectrum indicating formation of APX.

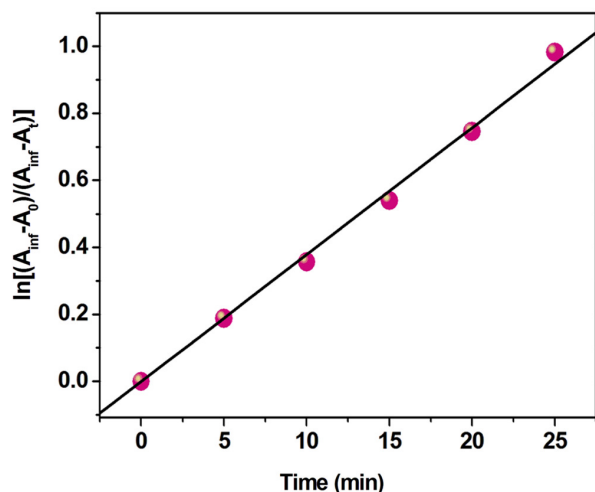
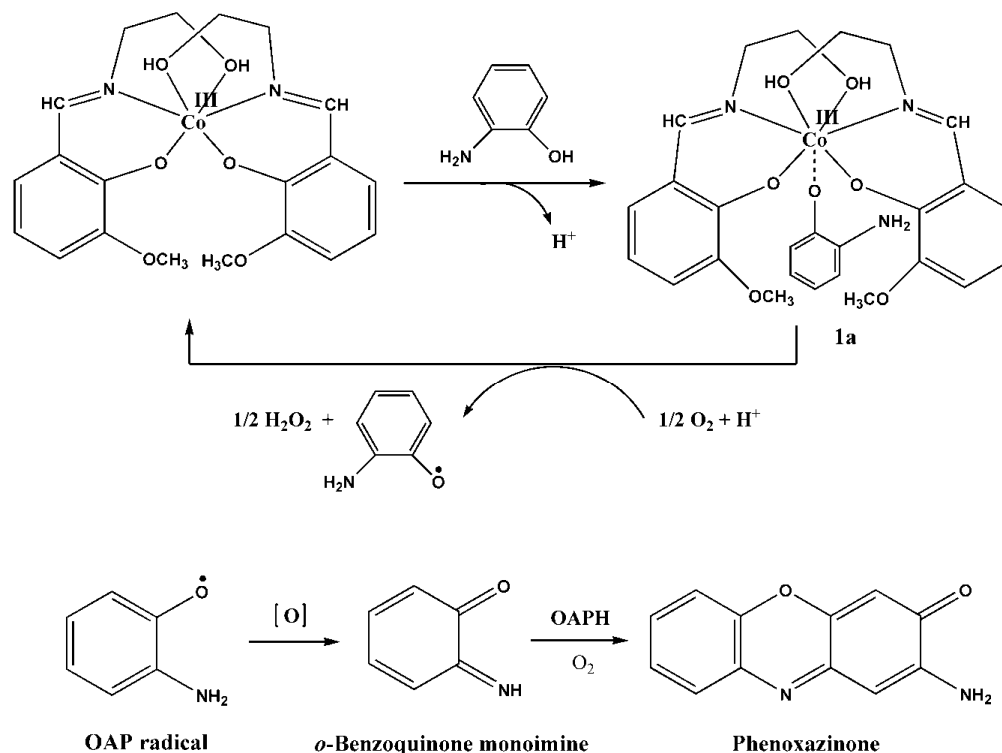


Fig. 4—A plot of the difference in absorbance (ΔA) versus time to evaluate the initial rate of the catalytic oxidation of OAPH by (I).

Enzymatic kinetic experiments, thermostated at 25 °C, were carried out with complex (I) and the substrate OAPH in MeOH and monitored UV-vis spectrophotometrically. The complex solution (0.04 mL, with constant concentration of 1×10^{-4} M),

was added to 2 mL of OAPH (concentration varied from 1×10^{-3} M to 1×10^{-2} M) to achieve the ultimate concentration of the complex as 1×10^{-4} M. The conversion of OAPH to APX was monitored with time at a wavelength of 427 nm for solutions in MeOH. The rate for each concentration of the substrate was determined by the initial rate method. The rate versus concentration of substrate data were analyzed on the basis of Michaelis-Menten approach of enzymatic kinetics to get the Lineweaver-Burk (double reciprocal) plot as well as the values of the various kinetic parameters, viz., V_{\max} , K_M and K_{cat} . The observed rate versus [substrate] plot in methanol solution as well as Lineweaver-Burk plot is given in Fig. 5. The kinetic parameters are listed in Table 1. The turnover number in methanol (K_{cat}) is found to be $2.83 \times 10^4 \text{ h}^{-1}$.

In the present study, we have reported the phenoxazinone synthase activity of a Co(III) complex reported previously by our group¹⁸. Kinetic investigation shows that the oxygenation



Scheme 3

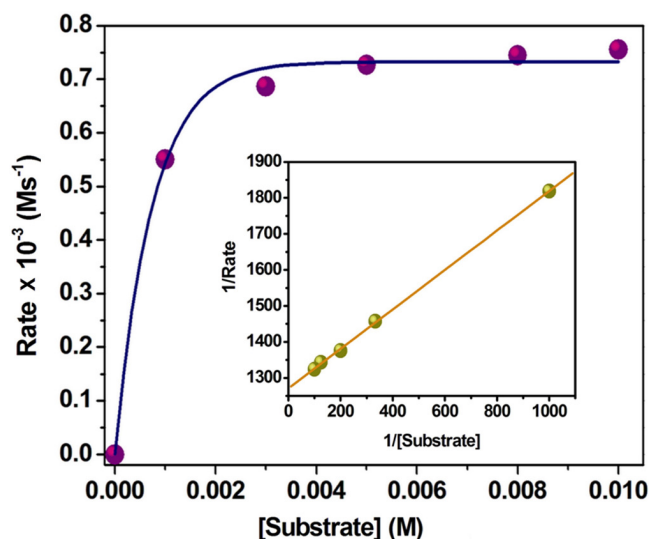


Fig. 5—Plot of rate versus [substrate] in presence of (1) in MeOH. [Inset: Lineweaver-Burk plot].

of *o*-aminophenol to phenoxazinone in presence of (1) proceeds through a first order reaction pathway. The reaction also follows Michaelis-Menten kinetics with appreciably high turnover number of $2.83 \times 10^4 \text{ h}^{-1}$, which is much higher than the value reported elsewhere^{15a,15c-e,16,17a}. Although some studies with the same activity

Table 1—Kinetic parameters for the oxidation of *o*-aminophenol in methanol catalyzed by (1)

| Parameter | Value | Std. error |
|-------------------------------------|-----------------------|-----------------------|
| $V_{\text{max}} (M \text{ s}^{-1})$ | 7.87×10^{-4} | 5.41×10^{-5} |
| $K_{\text{M}} (M)$ | 4.31×10^{-4} | 7.75×10^{-5} |
| $K_{\text{cat}} (\text{h}^{-1})$ | 2.83×10^4 | |

were found in the literature^{14,15b,17b}, but the evaluation of the turnover number has not been reported in these reports.

Supplementary data

Supplementary Data associated with this article, viz., Figs S1 and S2, and details on the spectrophotometric detection of H_2O_2 in the oxidation reaction, are available in the electronic form at [http://www.niscair.res.in/jinfo/ijca/IJCA_55A\(06\)681-685_SupplData.pdf](http://www.niscair.res.in/jinfo/ijca/IJCA_55A(06)681-685_SupplData.pdf).

Acknowledgement

RG sincerely thanks Department of Science & Technology, Government of West Bengal [No. 781(Sanc.)/ST/P/S&T/4G-4/2013 dated 04-12-2014] for financial assistance. MM thanks The University of Burdwan for the state funded fellowship.

References

- 1 Simándi L I, *Catalytic Activation of Dioxygen by Metal Complexes*, (Kluwer, Dordrecht) 1992.
- 2 Meunier E B, *Biomimetic Oxidations Catalyzed by Transition Metal Complexes*, (Imperial College Press, London) 2000.
- 3 (a) Solomon E I, Sundaram U M & Machonkin T E, *Chem Rev*, 96 (1996) 2563; (b) Lewis E A & Tolman W B, *Chem Rev*, 104 (2004) 1047; (c) Costas M, Mehn M P, Jensen M P & Que Jr L, *Chem Rev*, 104 (2004) 939.
- 4 Reedijk J, *Bioinorganic catalysis*, Dekker, New York, 1993.
- 5 (a) Mandal S, Mukherjee J, Lloret F & Mukherjee R, *Inorg Chem*, 51 (2012) 13148; (b) Koval I A, Selmececi K, Belle C, Philouze C, Saint-Aman E, Gautier-Luneau I, Schuitema A M, van Vliet M, Gamez P, Roubeau O, Lützen M, Krebs B, Lutz M, Spek A L, Pierre J-L & Reedijk J, *Chem Eur J*, 12 (2006) 6138; (c) Thio Y, Yang X & Vittal J J, *Dalton Trans*, 43 (2014) 3545; (d) Comba P, Martin B, Muruganatham A & Straub J, *Inorg Chem*, 51 (2012) 9214.
- 6 (a) Sanyal R, Zhang X, Kundu P, Chattopadhyay T, Zhao C, Mautner F A & Das D, *Inorg Chem*, 54 (2015) 2315; (b) Chattopadhyay T, Mukherjee M, Mondal A, Maiti P, Banerjee A, Banu K S, Bhattacharya S, Roy B, Chattopadhyay D J, Mondal T K, Nethaji M, Zangrando E & Das D, *Inorg Chem*, 49 (2010) 3121.
- 7 Simándi L I, Simándi T M, May Z & Besenyi G, *Coord Chem Rev*, 245 (2003) 85.
- 8 Barry C E, Nayar P G & Begley T P, *Biochemistry*, 28 (1989) 6323.
- 9 Jones G H & Hopwood D A, *J Biol Chem*, 259 (1984) 14151.
- 10 (a) Smith A W, Camara-Artigas A, Wang M, Allen J P & Francisco W A, *Biochemistry*, 45 (2006) 4378; (b) Barry C E, Nayar P & Begley T P, *J Am Chem Soc*, 110 (1988) 3333.
- 11 Hollstein U, *Chem Rev* 74 (1974) 625.
- 12 Katz E & Weissbach H, *J Biol Chem*, 237 (1962) 882.
- 13 Frei E, *Cancer Chemother Rep*, 58 (1974) 49.
- 14 Mukherjee C, Weyhermüller T, Bothe E, Rentschler E & Chaudhuri P, *Inorg Chem*, 46 (2007) 9895.
- 15 (a) Simándi L I, Barna T M, Korecz L & Rockenbauer A, *Tet Lett*, 34 (1993) 717; (b) Hassanein M, Abdo M, Gerges S & El-Khalafy S, *J Mol Catal A*, 287 (2008) 53; (c) Panja A & Guionneau P, *Dalton Trans*, 42 (2013) 5068; (d) Panja A, Shyamal M, Saha A & Mandal T K, *Dalton Trans*, 43 (2014) 5443; (e) Panja A, *Dalton Trans*, 43 (2014) 7760.
- 16 (a) Kaizer J, Baráth G, Csonka R, Speier G, Korecz L, Rockenbauer A & Párkányi L, *J Inorg Biochem*, 102 (2008) 773; (b) Mukherjee C, Weyhermüller T, Bothe E & Chaudhuri P, *CR Chimie*, 10 (2007) 313.
- 17 (a) Bakshi R, Kumar R & Mathur P, *Catal Commun*, 17 (2012) 140; (b) Simándi T M, Simándi L I, Györ M, Rockenbauer A & Gömöry Á, *Dalton Trans*, (2004) 1056.
- 18 Mitra M, Raghavaiah P & Ghosh R, *New J Chem*, 39 (2015) 200.
- 19 (a) Panja A, *Polyhedron*, 80 (2014) 81; (b) Panja A, *Polyhedron*, 79 (2014) 258.